

# ALKALI-ACTIVATION KINETICS OF PHOSPHORUS SLAG CEMENT USING COMPRESSIVE STRENGTH DATA

HOJJATOLLAH MAGHSOODLOORAD\*, #ALI ALLAHVERDI\*\*

\*Research laboratory of Inorganic Chemical Process Technologies, School of Chemical Engineering, Iran University of Science and Technology, Narmak 1684613114, Tehran, Iran

\*\*Cement Research Center, Iran University of Science and Technology, Narmak 1684613114, Tehran, Iran

#E-mail: ali.allahverdi@iust.ac.ir

Submitted June 15, 2015; accepted August 31, 2015

**Keywords:** Kinetics, Reaction order, Alkali-activation, Phosphorus slag

*In this research, through compressive strength data, the order and kinetics of alkali-activation of phosphorus slag activated with two compound activators of NaOH + Na<sub>2</sub>CO<sub>3</sub> and Na<sub>2</sub>CO<sub>3</sub> + Ca(OH)<sub>2</sub>, has been evaluated. The kinetics and order of alkali activation is a key factor to forecasting the mechanical behavior of alkali activated cement at different curing time and temperatures without carrying out experimental tests. The apparent activation energy was obtained as 35.6 kJ·mol<sup>-1</sup> and 60.7 kJ·mol<sup>-1</sup> for the two activators, respectively. Investigations proved that the alkali-activation kinetics of phosphorus slag resembles chemical reactions of second order. Moreover, the order of alkali-activation of phosphorus slag does not depend on the type of activator.*

## INTRODUCTION

Slag activation with alkalis under high pH condition (pH = 12 - 14) leads to producing high strength binders. These binders have a potential to be used instead of Portland cement due to their desirable properties as well as more environmental compatibility. In the production process of binders which are the result of alkali activation of slag, less amount of CO<sub>2</sub> is produced. Moreover, by production of these binders, industrial wastes, which are pollutant in some cases, are reused. Slag alkali-activation was reported in 1940 for the first time by Purdon [1]. Afterwards, Davidovits introduced geopolymer cements in 1979 [2]. By production of geopolymer cement, an alkali-activation technique has spread to materials, which contain reactive aluminosilicates like metakaolin, fly ash, etc.

A chemical reaction between slag and alkaline compounds like NaOH, KOH with/or without liquid sodium silicate results in the production of these kinds of binders [3]. Alkali-activation reactions include a set of complex chemical reactions in liquid-solid and solid-solid phases. These reactions are much more complicated than Portland cement hydration reactions [4]. For this reason, their kinetics has not yet been fully understood.

The conventional methods in forecasting mechanical behavior of cement mortar and concretes are mostly based on modeling the obtained experimental

results without taking the kinetics and order of hydration reactions into account. The study of kinetics and order of alkali activation provides a more in-depth insight to forecasting the mechanical behavior of alkali activated cement mortar and concretes [5-8]. This study helps in understanding the relationship between the amount of produced hydration products and for example compressive strength at different curing time and temperatures [6, 9-10]. These information are useful in estimating the mechanical behavior of cement mortar and concretes at different curing time and temperatures more carefully without carrying out experimental tests.

From Davidovits's standpoint, during the alkali activation process, a portion of present alumina and silica in the precursor is dissolved in an alkali environment. Subsequently a coagulated phase is formed because a reaction occurs between these materials. The coagulated phase is an intermediate compound between reactants and final products, and poly-condensation of this phase results in hydrated and polymerized cement compounds.

In studying the kinetics of these reactions, challenges like:

- 1) a chemical reaction between reactants in the solid phase and a thin liquid film, which is formed around particles [3],
- 2) products which are usually amorphous are not recognizable precisely [11-14],

3) an accurate measurement of the amount of products and non-reacted materials in specified time intervals is difficult, can be addressed.

Owing to these constraints, researchers consider the set of chemical changes that occurs during alkali activation, as a single overall reaction, in which reactants are converted to products [4, 8, 15]. Based on this simplification, researchers have been able to compute apparent activation energy for the whole process by means of isothermal calorimetric studies. For this purpose, the rate of heat release in the alkali activation process at definite and controlled temperatures is measured, then the activation energy of the reaction is calculated by utilizing Arrhenius equation [15-16]. Exploitation of the isothermal calorimetric method, nevertheless, is hard to approach because of complication, relatively high expenses and inaccessibility of the equipment. Therefore, simple and cheap methods for these kinds of studies have been always sought. Using compressive strength data is one of these methods. Compressive strength test is a common and preliminary experiment to assess inorganic binders.

In this research, the apparent activation energy as well as the order of alkali-activation of phosphorus slag was calculated through compressive strength of mortar specimens, which were cured at definite temperatures. Moreover, compressive strength data has been applied for the first time to investigate the order of alkali activation. Since formation of polymeric and hydrated compounds leads to compressive strength, thereby the amount of produced cementitious compounds and correspondingly the order of the reaction can be computed so long as the compressive strength of specimens at definite temperatures and time intervals is measured and compared to standard ultimate compressive strength.

In addition to investigation of alkali-activation kinetics of phosphorus slag, compressive strength data of this kind of cement is evaluated in this study. Possibility of producing a suitable binder from this slag has been observed in recent studies [3, 17-18]. Phosphorus slag is an industrial waste in the manufacturing process of yellow phosphor. It contains little amounts of phosphorus pentoxide, which significantly increases hardening time of Portland cement [3, 17]. Presence of phosphorus pentoxide in this substance, makes its utilization as an additive in Portland cement either impossible or severely restricted. Therefore, in order to reuse this industrial waste, suitable methods should be found in particular for countries which produce enormous volume of this waste material. Statistics reveal that in China 16 million ton of phosphorus slag was produced in 2006, approximately [19].

Table 1. Chemical composition of phosphorus slag.

Oxide	SiO <sub>2</sub>	Al <sub>2</sub> O <sub>3</sub>	Fe <sub>2</sub> O <sub>3</sub>	CaO	MgO	P <sub>2</sub> O <sub>5</sub>	K <sub>2</sub> O	Na <sub>2</sub> O	SO <sub>3</sub>	Cl	LOI
wt. %	38.42	7.65	0.90	45.14	2.60	1.50	0.56	0.43	ND	ND	1.87

## EXPERIMENTAL

### Materials

Alkali materials such as sodium hydroxide (NaOH, 99 %, Merck), calcium hydroxide (Ca(OH)<sub>2</sub>, 99 %, Merck), sodium carbonate (Na<sub>2</sub>CO<sub>3</sub>, 99 %, Merck) and distilled water were used. In this experiment, phosphorus slag was prepared from a phosphoric acid production plant, which is located in the south east of Tehran province in Iran. The chemical composition of this slag was determined in accordance with ASTM C 114 and C 311 standards [20-21]. The determination procedures given in these standards for chemical composition of supplementary cementing materials and blended cements with insoluble residue greater than 1 % are based on the sodium carbonate fusion of the sample followed by classical analytical procedures (either gravimetric and volumetric) for silicate materials as given in ASTM C 114 [20]. Table 1 shows the chemical composition of the phosphorus slag. With regard to the chemical composition, this slag is neutral with a basicity coefficient of ( $K_b = (\text{CaO} + \text{MgO})/(\text{SiO}_2 + \text{Al}_2\text{O}_3)$ ) 1.04. X-ray diffraction pattern of phosphorus slag is presented in Figure 1. As can be noticed, the predominant part of this material is amorphous and just a mere proportion of crystalline magnesium oxide (periclase) exists in it. In order to prepare mortar specimens, standard silica sand (ASTM C 778 [22]) was utilized.

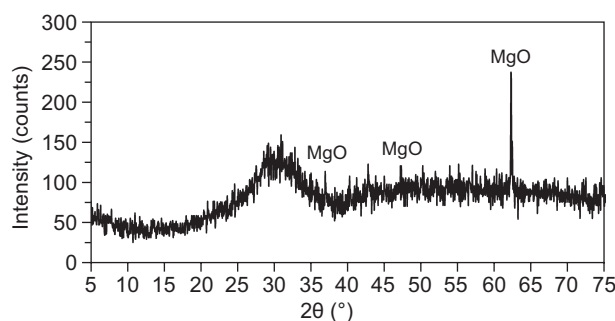


Figure 1. X-ray diffraction pattern of phosphorus slag.

### Experimental methods

In the first step, granulated phosphorus slag was ground in a laboratory ball mill (380 mm long and 110 mm in diameter) to reach Blaine fineness of  $3000 \pm 50 \text{ cm}^2 \cdot \text{g}^{-1}$ . Afterwards, a laser diffraction particle size analysis was used to determine the size distribution of

ground phosphorus slag (Figure 2). Based on obtained data, geometric mean diameter of ground slag was 10.16  $\mu\text{m}$ .

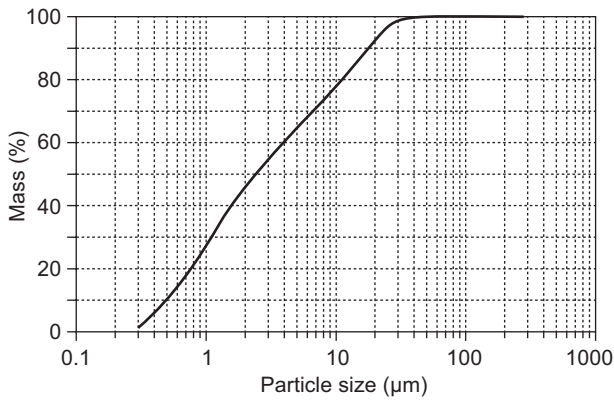
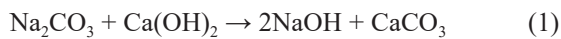


Figure 2. Particle size distribution of ground phosphorus slag.

According to Table 2, two different compound alkali activators, which consist of  $\text{NaOH} + \text{Na}_2\text{CO}_3$  and  $\text{Na}_2\text{CO}_3 + \text{Ca}(\text{OH})_2$  were applied to activate phosphorus slag. To prepare activators, the required distilled water on the base of water-to-slag ratio (water/slag = 0.455) along with other substances ( $\text{Ca}(\text{OH})_2$ ,  $\text{NaOH}$ ,  $\text{Na}_2\text{CO}_3$ ) were weighted. In activator No.1, a proportion of required alkali was supplied with sodium carbonate, thus reducing the consumption rate of sodium hydroxide. In the 2<sup>nd</sup> activator, A reaction between  $\text{Na}_2\text{CO}_3$  and  $\text{Ca}(\text{OH})_2$  according to Equation 1, produces the required amount of alkali in the form of sodium hydroxide. Consistent with Equation 1 and the weight ratio of dry slag, the required amount of  $\text{Na}_2\text{CO}_3$  and  $\text{Ca}(\text{OH})_2$  in activator No. 2 was set to produce equivalent quantity of 5 % sodium hydroxide in cementitious mixture.



In order to prepare the activator No.1, sodium hydroxide was dissolved in distilled water and consequently sodium carbonate was added to the solution, together with stirring until complete dissolution. For the 2<sup>nd</sup> activator, likewise, sodium carbonate was dissolved in distilled water, followed by calcium hydroxide addition, along with 20 minutes of stirring at the speed of 100 rpm.

In consonance with ASTM C 109 [23] standard, mortar specimens were made. The start of this step was mixing slag and silica sand with weight ratio of 1 to 2.75. Thereupon, prepared activators were added to the mixture of sand and slag accompanied by 5 minutes at the speed of 50 rpm of mixing until a perfect homogenized cementitious mixture was prepared. Subsequently, cementitious mixtures were molded into stainless steel  $5 \times 5 \times 5$  cm cubic molds by vibration, and then kept for 24 hours in an environment of more than 95 % relative humidity at temperature of 16, 25 and 35°C (according to ASTM C 1074 [10]; standard practice for

estimating concrete strength by the maturity method) with an accuracy of  $\pm 1^\circ\text{C}$  to become hardened enough. These temperatures are proposed by ASTM C 1074 [10] standard for determining the activation energy of cement mortars. After this period, hardened specimens were removed from molds and cured at the same condition until the compressive strength testing time. Compressive strength test was conducted in compliance with ASTM C 109 [23] standard at 12 hours, 1, 2, 4, 8, 16 and 32 days intervals. Three specimens were used in each measurement and upshot was the mean of them. For compressive strength, the accuracy was  $\pm 5\%$ .

Table 2. Chemical composition of alkali-activators.

No.	Type of activator	Composition (% by weight of slag)
1	$\text{NaOH} + \text{Na}_2\text{CO}_3$	$\text{NaOH}$ : 3 % $\text{Na}_2\text{CO}_3$ : 1 %
2	$\text{Na}_2\text{CO}_3 + \text{Ca}(\text{OH})_2 \rightarrow 2\text{NaOH} + \text{CaCO}_3$	$\text{NaOH}$ : 5 %

To determine particle size distribution of phosphorous slag, the *Fritsch* Laser Particle Sizer (analysette 22 compact, Germany) was utilized. Complementary laboratory techniques including XRD, SEM and FTIR were also applied. The X-ray diffraction pattern of phosphorus slag was recorded on a Philips Expert diffractometer using  $\text{CuK}\alpha$  radiation at 40 kV and 30 mA. The tests was run in a 2 h range of 5 - 75° at a scanning rate of  $2^\circ \cdot \text{min}^{-1}$ , with a deliverance slit of  $1^\circ$ , an anti-scatter slit of  $1^\circ$ , and a receiving slit of 0.01 mm. FTIR spectra were collected using a Nicolet 740 FTIR spectrometer in transmittance mode from 500 to 4500  $\text{cm}^{-1}$  using standard KBr technique (0.5 mg sample with 250 mg KBr). All spectra were obtained with a sensitivity of 4  $\text{cm}^{-1}$  and 64 scans per spectrum taken. The microstructure of the mortar specimens were investigated using BSE mode of a TESCAN VEGA II Scanning Electron Microscope at 30 kV. For SEM studies, a number of mortar specimens were cut into halves to expose internal regions. Suitable halves were then impregnated with epoxy resin, polished, and coated with carbon.

## RESULTS AND DISCUSSIONS

### Compressive strength of specimens

Compressive strengths of the two cement mixtures at each of three examined temperatures are displayed in Table 3. It is discerned that both cement mixtures have shown proper compressive strength. Reaching 50 MPa in compressive strength at 25°C, which is close to the standard temperature  $23 \pm 2^\circ\text{C}$  (ASTM C 109 [23]) for compressive strength test, is attainable.

These results exhibit appropriate quality of the slag as well as the proper use of activators to produce quality cement. According to Table 3, moreover, compressive strength of cement mixtures is a function of temperature so that an increase in temperature gives rise to it. Both cement mixtures show higher rates of compressive strength development at earlier ages of curing and at higher temperatures. In the first 8 days, 2 - 2.5 times increase in compressive strength is accompanied with increase in temperature per each 10°C; on the contrary, in next days through the 32<sup>nd</sup> day, this rate decreases to 1.3 - 1.5 times, approximately.

The reason of increasing compressive strength with temperature rise is associated with the effect of temperature on the kinetics of alkali-activation process in these cement mixtures. In chemical reactions, an increase in temperature typically causes a speedup in the rate of reaction, together with formation of more products [3]. In the cement mixtures, more products signify higher compressive strength. Nonetheless, a temperature impact on compressive strength is greater in the first days because of the intrinsic nature of these reactions, which is special kinds of solid-liquid and solid-solid [24]. In the first days, cement mixtures involve higher concentration of activators and un-reacted slag. In this period, therefore, the chemical reaction is more influenced by temperature and rising temperature causes a higher build-up of compressive strength.

Table 3. Compressive strength (MPa) development at different temperatures.

	Time (day)	Temperature (°C)		
		16°C	25°C	35°C
Mix 1	0.5	2.8	6.9	11.7
	1	5.5	10.0	29.9
	2	11.7	23.4	45.4
	4	18.2	31.6	53.6
	8	21	39.4	63.6
	16	31.6	43.3	66.3
	32	34.0	51.3	73.0
Mix 2	0.5	3.8	6.5	11.7
	1	8.3	12.4	27.8
	2	12.4	23.4	39.9
	4	15.3	27.8	48.8
	8	20.3	33.0	52.6
	16	28.5	43.7	57.1
	32	32.7	49.5	63.9

As the time passes, on the one hand the amount of un-reacted activator and slag decreases and on the other hand, activator should diffuse through solid phase products to reach the un-reacted slag in order to make progress of the reaction possible. Hence after 8 days, the reaction rate, and consequently the compressive strength of the cement mixtures undergo minor changes especially at higher temperatures.

#### Apparent activation energy

As it was mentioned, complex reactions are involved in the alkali-activation process of slag; ergo, it is not viable to study each of them separately. On this account, to simplify the investigation of kinetics of alkali-activation process, all involved reactions in this process are considered as a single overall reaction, which is similar to the following equation:



Entire reactants as well as all cementitious products, which are involved in the process of alkali activation of phosphorus slag, are represented as reactant and product in Equation 2, respectively. Moreover, for further investigations on alkali-activation kinetics of phosphorus slag, along with temperature impacts on the formation process of cementitious products, Arrhenius equation (Equation 3) was used. Arrhenius equation (Equation 3) is the base for one of the most common and accurate procedures to explain how temperature affects the kinetics of many chemical and physical processes [15].

$$K(T) = K_0 \cdot \text{Exp}\left(-\frac{E^a}{R \cdot T}\right) \quad (3)$$

where  $T$  is the absolute temperature (K),  $E^a$  is the apparent activation energy ( $\text{J} \cdot \text{mol}^{-1}$ ),  $R$  is the gas constant, which equals 8.314. This equation can be rewritten in the following form:

$$\ln(K(T)) = \ln(K_0) - \frac{E^a}{R \cdot T} \quad (4)$$

This form of Arrhenius equation is more beneficial because the quantity of  $(E^a)/(R \cdot T)$  can be obtained from the diagram of  $\ln(K)$  versus  $1/T$ . Based upon the ASTM C1074 [10] standard, compressive strength was applied to find the reaction constant ( $K$ ) and apparent activation energy [10]. A three-stage approach was taken to acquire apparent activation energy.

*Step 1:* at each temperature, the last four data of compressive strength were used and inverse of compressive strength was plotted versus inverse of time. Afterwards, the slope and the intercept of a fitted curve were calculated. In this case, the intercept should be inverted to result in ultimate compressive strength ( $S_u$ ) at the specified temperature. For the last four experiments at each of three curing temperatures, the inverse of compressive strength was delineated against the inverted time, which is displayed in Figures 3 and 4 for the first and the second cement mixtures, respectively. It is evident that alterations in all cases are almost linear; moreover, linear equations can be utilized to fit the change rate.

By making use of linear equations of changes, the amount of  $S_u$  for both cement mixtures was reckoned. Resultant quantities for  $S_u$  are demonstrated in Table 4.

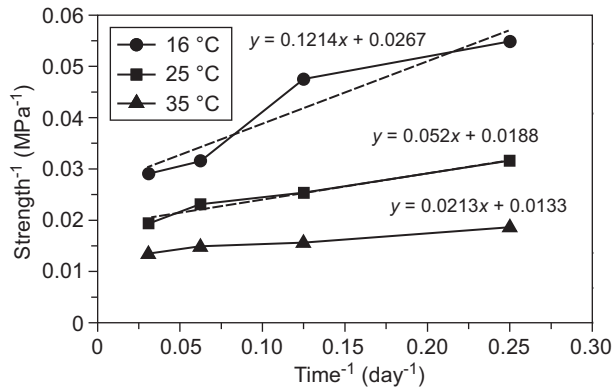


Figure 3. Inverted compressive strength versus inverse of curing time of cement mixture No.1 for the last four measurements.

Table 4.  $S_u$  values for both cement mixtures at different temperatures.

	Temperature (°C)	$S_u$ (MPa)
Mix 1	16	38.46
	25	55.56
	35	76.92
Mix 2	16	38.46
	25	55.56
	35	66.67

According to Table 4, an increase in temperature causes growth in ultimate compressive strength of both cement mixtures. Supplying more energy together with rising temperature bring about further and better proceeding of involved reactions in the activation process and more cementing compounds are produced. A step up in the production of cementing compounds causes increase in the compressive strength of the specimens. Additionally, some researchers have investigated the effect of curing temperature rise on amplification of compressive strength. These researchers have expressed that based on the type and the amount of activator, a 10-degree-rise in the curing temperature, may boost the compressive strength up to double [3].

*Step 2:* For each temperature, data of compressive strength for the four earliest test ages was considered and through using Equation 5, the amount of  $A$  was computed.

$$A = \frac{S}{S_u - S} \quad (5)$$

The compressive strength (MPa) at the test time is shown as  $S$  in Equation 5. The “ $A$ ” parameter was calculated by making use of Equation 5; thereafter, these values were tabulated and presented in Table 5.

*Step 3:* For each temperature, “ $A$ ” values were plotted versus time. The slope of lines, which were fitted on data, is equivalent to the reaction constant ( $K$ ). Figures 5 and 6 display the diagram of “ $A$ ” parameter changes versus time for cement mixtures 1 and 2, respectively.

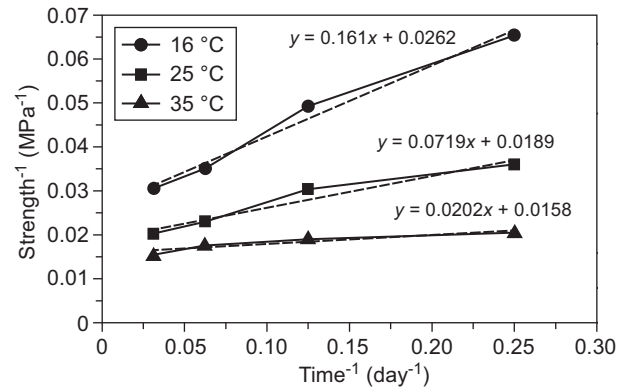


Figure 4. Inverted compressive strength versus inverse of curing time of cement mixture No.2 for the last four measurements.

Table 5. Values of “ $A$ ” parameter.

	Time (day)	Temperature (°C)		
		16°C	25°C	35°C
Mix 1	0.5	0.077006	0.141227	0.179158
	1	0.166861	0.218676	0.636075
	2	0.436524	0.72637	1.438281
	4	0.900012	1.321532	2.301692
Mix 2	0.5	0.109032	0.133225	0.212581
	1	0.273074	0.286587	0.717199
	2	0.474383	0.72637	1.488336
	4	0.660354	1.004761	2.733956

The  $K$  parameter values are summarized in Table 6 for both cement mixtures at each of three temperatures.

Table 6.  $K$  values of cement mixtures 1 and 2.

	Temperature (°C)	$K$
Mix 1	16	0.238
	25	0.349
	35	0.593
Mix 2	16	0.149
	25	0.249
	35	0.706

As it is obvious, an increase in the reaction constant is the outcome of rising temperature in such a way that almost for every 10°C increase in curing temperature, the reaction constant of cement mixture 1 and cement mixture 2 become 1.5 - 1.7 and 1.7 - 2.8 times more than before, respectively. Extra changes of  $K$  value as a result of temperature change in the second cement mixture interprets that further reaction between  $\text{Na}_2\text{CO}_3$  and  $\text{Ca}(\text{OH})_2$  has occurred. During the activator solution preparation for cement mixture 2, this reaction has not been completed. Formation of solid phase  $\text{CaCO}_3$ , leads the reaction to proceed spontaneously at its beginning whereas increasing the concentration of produced  $\text{NaOH}$ , turn this reaction into an endothermic over time [25-27].

During the activation process of slag, consuming NaOH, together with providing required heat through activation energy are the two means that make this reaction to be completed gradually. In this cement mixture, therefore, the required heat for faster completion of the reaction is supplied by increasing curing temperature. Quicker finish of the above reaction speeds up the activation

reaction of slag. Hence, reaction constant for cement mixture 2 is more impressed by curing temperature.

After calculation of  $K$  at each temperature, the value of apparent activation energy was computed through plotting the diagram of  $\ln(K)$  versus  $T$  (in Kelvin unit) and finding the slope of fitted line. The apparent activation energy may be achieved from the slope of the fitted line,

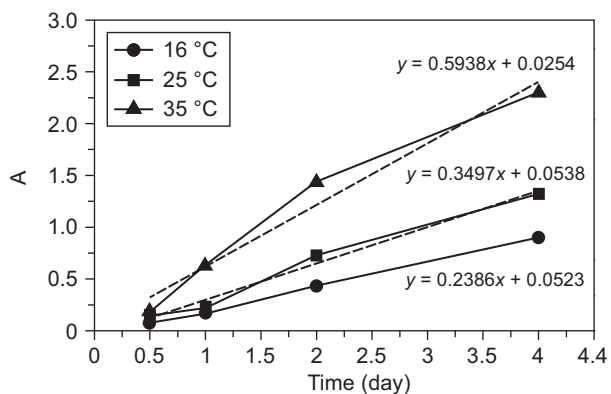


Figure 5. “A” parameter changes diagram versus time for cement mixture 1.

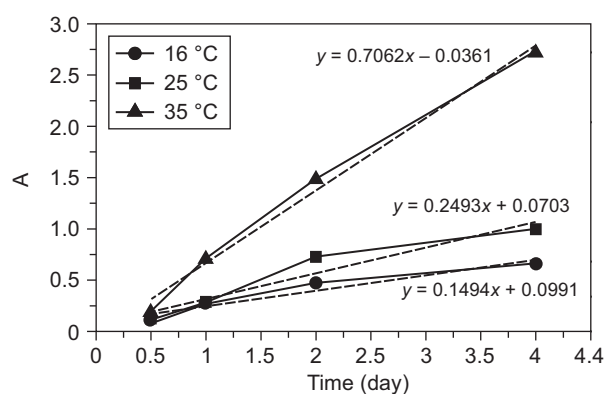


Figure 6. “A” parameter changes diagram versus time for cement mixture 2.

Table 7. The apparent activation energy of Portland cement and alkali-activated blast-furnace and phosphorus slags.

	$E^a$ (kJ·mol <sup>-1</sup> )	Type	Activator	reference
Roy and Idorn	44.3	OPC	–	[28]
Ezziane et al.	24.4	OPC	–	[29]
Shindler	45.2	OPC	–	[30]
Ma et al.	39.0	OPC	–	[31]
Wu et al.	44.31	OPC	–	[4]
Huanhai et al.	53.63	Alkali-activated blast furnace slag	Liquid sodium silicate with Ms = 1	[8]
Fernandez-Jimenez and Puertas	57.6	Alkali-activated blast furnace slag	Liquid sodium silicate with Na <sub>2</sub> O = 4 %	[24]
This work	35.6	Alkali-activated phosphorus slag	3 % NaOH + 1 % Na <sub>2</sub> CO <sub>3</sub>	–
	60.7	Alkali-activated phosphorus slag	Produced 5 % NaOH by Na <sub>2</sub> CO <sub>3</sub> + Ca(OH) <sub>2</sub> → 2NaOH + CaCO <sub>3</sub>	–

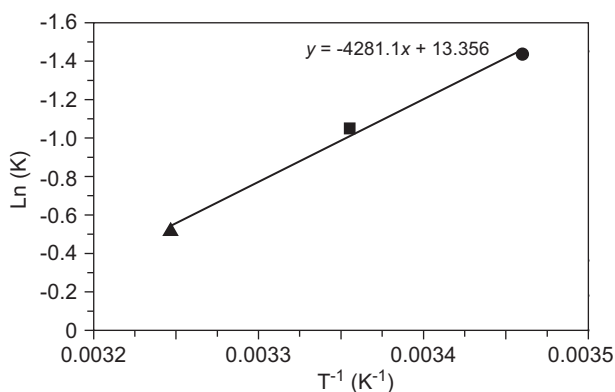


Figure 7. The  $\ln(K)$  diagram in terms of inverse curing temperature for cement mixture 1.

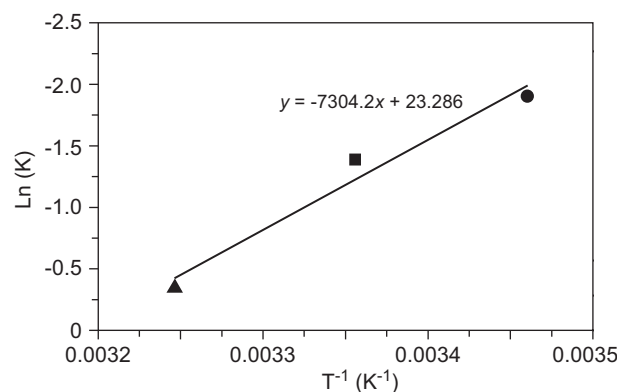


Figure 8. The  $\ln(K)$  diagram in terms of inverse curing temperature for cement mixture 2.

which is equal to  $E_a/R$ . The diagram of  $\ln(K)$  in terms of inverse curing temperature is displayed in Figures 7 and 8 for cement mixtures 1 and 2 in order.

As per these Figures, the amount of  $E_a/R$  for cement mixtures 1 and 2 is equal to 4281 K and 7304 K, respectively, and multiplying these amounts by the gas constant ( $R = 8.314 \text{ J}\cdot\text{K}^{-1} \text{ mol}^{-1}$ ) yields 35.6 and 60.7  $\text{kJ}\cdot\text{mol}^{-1}$  as the apparent activation energy of cement mixtures 1 and 2, respectively. As it is regarded, the amount of activation energy for alkali-activation of phosphorus slag depends on the type of activator. Making comparison between the calculated apparent activation energy in this research and reported values in other researches for Portland cement and alkali-activated blast-furnace slag (Table 7) clarifies that the apparent activation energy for cement mixture 1 is nearly equivalent to that Portland cement. For the cement mixture 2, however, this amount is much greater and almost equals the apparent activation energy of blast-furnace slag, which is activated by a sodium silicate solution and its combination with sodium hydroxide.

Order of reaction rate

In order to find the reaction rate order, concentration changes for the reactant ( $A$ ) (regardless of real values) with respect to reaction time and temperature should be specified for both cement mixtures. Due to the fact that the compressive strength demonstrates the rate of produced cementing compounds, and also higher compressive strength indicates that the reaction brings about more product ( $B$ ), thus through utilizing compressive strength at each time as well as comparing this value with ultimate compressive strength in each temperature ( $S_u$  in Table 4), the fractional conversion can be calculated (Equation 6).

$$x_B = \frac{S}{S_u} \tag{6}$$

Moreover, by taking the general Equation (Equation 2) of activation process into consideration, the fractional conversion of the reactant is equivalent to the fractional conversion of the product, in other words:

$$x_A = x_B \tag{7}$$

Now, the reactant concentration at each moment can be calculated with respect to the following formula:

$$C_A = C_{A0} \cdot (1 - x_A) \tag{8}$$

In Equation 8, the reactant concentration at different times and at the beginning and also the fractional conversion are expressed as  $C_A$ ,  $C_{A0}$  and  $x_A$ , respectively. By assuming the initial reactant concentration as a base to be equivalent to 1  $\text{g}/(1 \text{ cm}^3)$ , its alterations at definite time and temperatures for both cement mixtures can be calculated (Table 8).

Table 8. Fractional conversion and reactant concentration for both cement mixtures (initial reactant concentration is assumed as 1  $\text{g}\cdot\text{cm}^{-3}$ ).

Time (day)	Temperature ( $^{\circ}\text{C}$ )						
	$x_A$			$C_A (\text{g}\cdot\text{cm}^{-3})$			
	16 $^{\circ}\text{C}$	25 $^{\circ}\text{C}$	35 $^{\circ}\text{C}$	16 $^{\circ}\text{C}$	25 $^{\circ}\text{C}$	35 $^{\circ}\text{C}$	
Mix 1	0.5	0.07	0.12	0.15	0.93	0.88	0.85
	1	0.14	0.18	0.39	0.86	0.82	0.61
	2	0.30	0.42	0.59	0.70	0.58	0.41
	4	0.47	0.57	0.70	0.53	0.43	0.30
	8	0.55	0.71	0.83	0.45	0.29	0.17
	16	0.82	0.78	0.86	0.18	0.22	0.14
Mix 2	0.5	0.10	0.12	0.18	0.90	0.88	0.82
	1	0.21	0.22	0.42	0.79	0.78	0.58
	2	0.32	0.42	0.60	0.68	0.58	0.40
	4	0.40	0.50	0.73	0.60	0.50	0.27
	8	0.53	0.59	0.79	0.47	0.41	0.21
	16	0.74	0.79	0.86	0.26	0.21	0.14
32	0.85	0.89	0.96	0.15	0.11	0.04	

When the reactant concentration is obtained, the calculation of the reaction rate order is possible. In this study, the reaction rate was assumed to be in simple form (Equation 9). In general, the reaction rate of such reactions amounts to 0, 1 and or 2 [9]. These orders should be checked separately to determine the reaction rate order.

$$\text{Rate} = -\frac{dC_A}{dt} = K \cdot C_A^n \tag{9}$$

Evaluation of the zero<sup>th</sup>-order

When the order is zero, the reaction rate is independent of the reactant concentration. Thus:

$$\text{Rate} = -\frac{dC_A}{dt} = K \cdot C_A^0 = K \tag{10}$$

For this reason, the diagram of the reactant concentration change versus time should be linear. Figures 9 and 10 display reactant ( $A$ ) concentration changes for each of the two cement mixtures. Because of non-linearity in concentration changes, the reaction rate could not be a zero-order one.

Evaluation of the first order

If the order of the activation reaction equals 1, the following equation must hold true:

$$\text{Rate} = -\frac{dC_A}{dt} = K \cdot C_A \tag{11}$$

Consequently, it can be written:

$$-\frac{dC_A}{C_A} = K \cdot dt \tag{12}$$

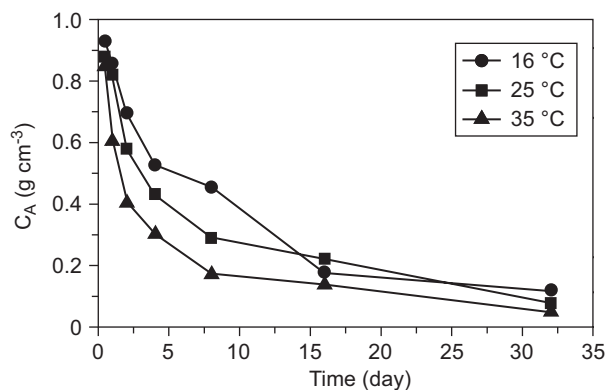


Figure 9. Reactant concentration changes versus time in cement mixture 1.

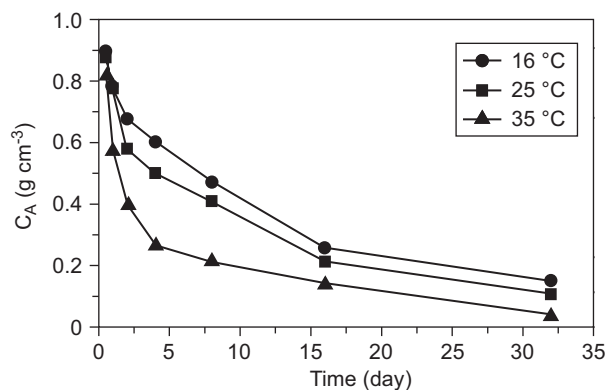


Figure 10. Reactant concentration changes versus time in cement mixture 2.

Integration of Equation 12 results in the following equations:

$$C_A = C_{A0} \cdot \exp(-K \cdot t) \quad (13)$$

or:

$$\ln(C_A) = \ln(C_{A0}) - K \cdot t \quad (14)$$

With respect to Equation 14, the reaction order is equivalent to one, provided that the natural logarithmic changes of reactant concentration shows linearity when plotted against time and in this state by converting the slope to its negative amount,  $K$  will be gained. Natural logarithmic of reactant concentration ( $A$ ) is plotted versus time and presented in Figures 11 and 12 for cement mixtures 1 and 2, respectively.

Figures 11 and 12 bring this subject to notice that at the two temperatures of 16°C and 25°C changes in natural logarithm of reactant ( $A$ ) concentration versus time can be considered linear, nevertheless, at 35°C the respective trend for both cement mixtures is not linear. In this research, simple equations, which are used for homogenous equation (Equation 9) as well as Arrhenius equation were applied to examine the reaction rate, hence it can be mentioned that the reaction rate is not in the first order, because by considering these assumptions, the temperature change does not affect the reaction rate order. The second order, therefore, should be assessed.

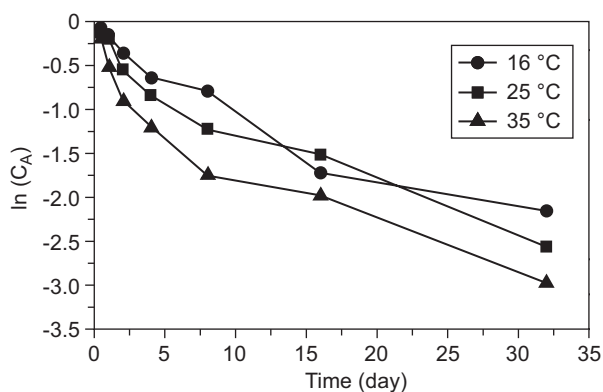


Figure 11. Changes in natural logarithm of reactant ( $A$ ) concentration versus time for cement mixture 1.

#### Evaluation of the second order

The Equation 15 holds true for the second order reactions:

$$\text{Rate} = -\frac{dC_A}{dt} = K \cdot C_A^2 \quad (15)$$

From Equation 15:

$$-\frac{dC_A}{C_A^2} = K \cdot dt \quad (16)$$

Through integrating Equation 16:

$$\frac{1}{C_A} = \frac{1}{C_{A0}} + K \cdot t \quad (17)$$

According to Equation 17, if the change of inverted reactant concentration is linear over time, the reaction is of the type second order and the  $K$  value equals the slope of change. Change in inverse of reactant ( $A$ ) concentration versus time for cement mixtures 1 and 2 are displayed in Figures 13 and 14.

Regarding Figures 13 and 14, the alteration of inverted reactant concentration versus time at each of the three temperatures is almost linear with negligible error. Therefore, based on considered assumptions, it can be claimed that the reaction rate of phosphorus slag alkali

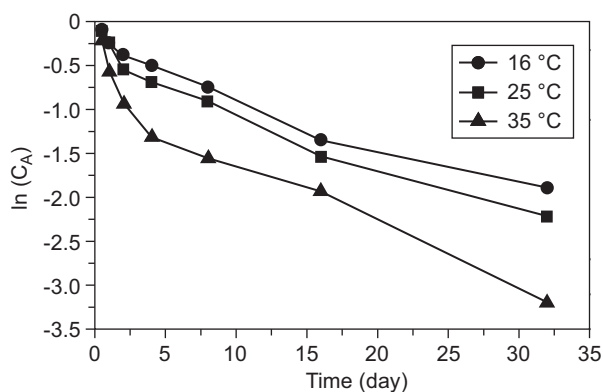


Figure 12. Changes in natural logarithm of reactant ( $A$ ) concentration versus time for cement mixture 2.

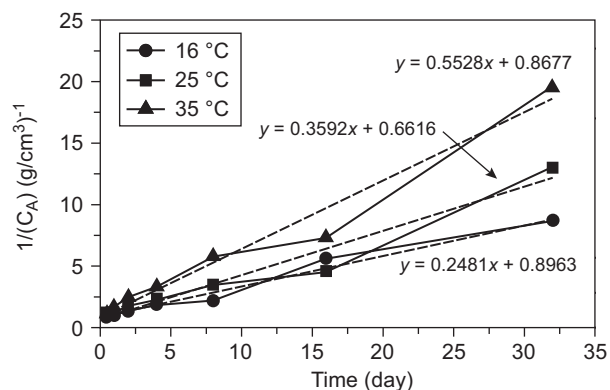


Figure 13. Change in inverse of reactant (A) concentration versus time for cement mixture 1.

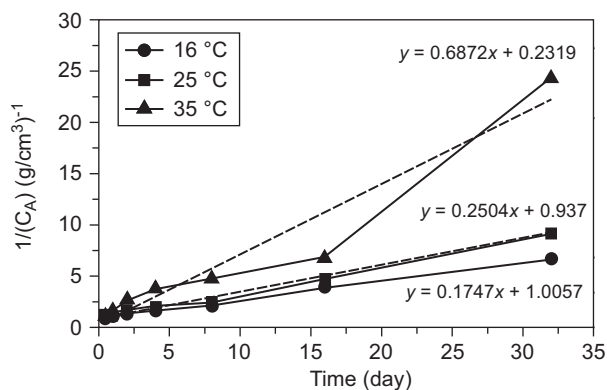


Figure 14. Change in inverse of reactant (A) concentration versus time for cement mixture 2.

activation is almost similar to second order chemical reactions and it does not rely on the type of activator. From Fernandez-Jimenez and Puertas point of view, molecular diffusion takes control of the kinetics of the slag activation process in case of having the second order reaction rate [24]. Owing to the presence of several reactants in solid and liquid phases instead of one reactant in the real condition, the second order reaction bears a meaning that reactants in the liquid phase should diffuse in the surrounded thin liquid film of slag as well as solid products in order to approach un-reacted slag to proceed the activation reaction. Equation of lines, which were fitted on presented data in Figures 13 and 14, results in  $K$  values, which are tabulated in Table 9. By drawing an analogy between  $K$  values in Table 6 and Table 9, it can be concluded that  $K$  values, which were calculated on the base of compressive strength, are approximately equivalent to computed values through ASTM C 1074. This subject introduces the method whereby compressive strength is utilized to evaluate the alkali-activation kinetics of slag with a close approximation.

Table 9.  $K$  values and  $R^2$  of fitted curves for cement mixtures 1 and 2.

	Temperature (°C)	$K$	$R^2$
Mix 1	16	0.248	0.98
	25	0.359	0.96
	35	0.552	0.97
Mix 2	16	0.174	0.99
	25	0.250	0.94
	35	0.687	0.93

#### FTIR and SEM studies

In almost all cases, the hydration products in alkali activated slag cements are completely amorphous and XRD technique is not useful for phase studies [11-12, 17, 32-34]. We, therefore, used FTIR Spectroscopy method to investigate bond structures in the formed

hydration products. Figure 15 shows the obtained FTIR spectroscopy results for the two cement mixtures cured at different temperature for 32 days. As seen, all the FTIR spectra are very similar except the broad peak in the wavelength of  $1000\text{ cm}^{-1}$ . This peak is related to Si-O bond vibrations in various structures ( $Q^n$ ,  $n = 0-4$ ) in C-S-H and/or C-A-S-H phases as confirmed by other researchers [35-36]. As can be noticed, this peak has transferred to slightly lower wavelengths and become sharper with increasing curing temperature. Transfer of this peak to lower wavelengths is an indication of increase in the polymerization degree of hydration products. The increase in curing temperature, therefore, not only increases the extent of progress in hydration reactions in general, but also increases the polymerization degree of hydration products.

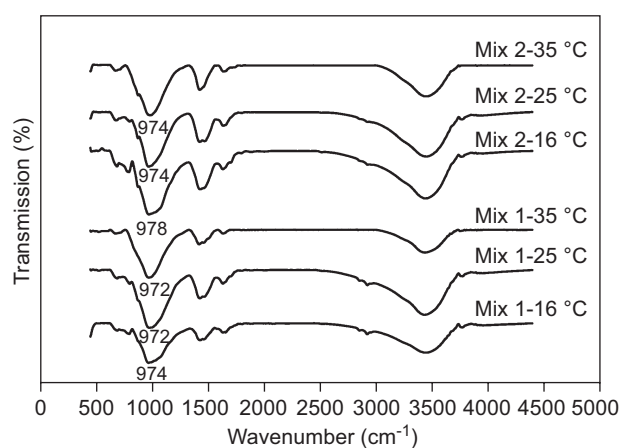


Figure 15. FTIR spectra of the two cement mixtures cured at different temperatures for 32 days.

Figure 16 shows the SEM images prepared from the microstructures of 32-day hardened mortar specimens cured at different temperatures at the same magnification of 200 times. As seen, the general microstructure is composed of a composite matrix in which un-reacted slag particles with straight edges and sharp corners are

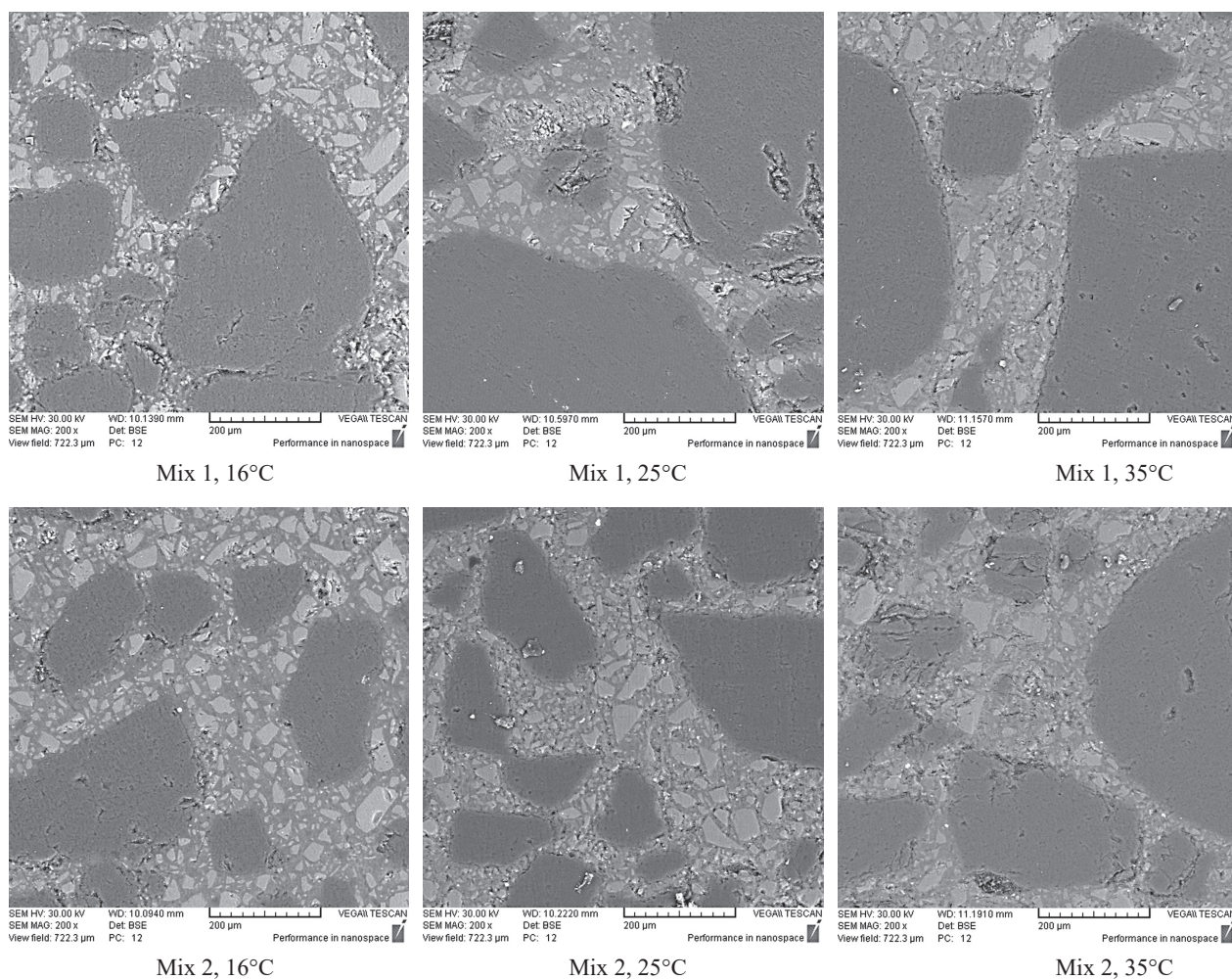


Figure 16. SEM images from the microstructure of 32-day hardened mortar specimens cured at different temperatures.

embedded. The microstructures developed at different temperatures seem very similar. A careful comparison of the images, however, reveals the differences between the microstructures developed at different curing temperatures. It seems that increasing the curing temperature from 16°C to 35°C decreases the number of un-reacted slag particles. The shape of the un-reacted slag particles also seems to be changed. Many of the un-reacted slag particles have lost their straight edges and sharp corners and un-reacted slag particles with round edges and corners can also be observed. These changes in the developed microstructures are due to the involvement of a higher proportion of the slag in the hydration reactions at higher curing temperatures.

## CONCLUSION

- Resultant compressive strength due to alkali-activation of phosphorus slag by means of two compound activators  $\text{NaOH} + \text{Na}_2\text{CO}_3$  and  $\text{Na}_2\text{CO}_3 + \text{Ca}(\text{OH})_2$  demonstrates that the compressive strength of cement mixtures is a function of temperature and per each

10°C rise in curing temperature, the compressive strength of cement mortars increases by 1.5 times on average.

- Obtained results from investigations on apparent activation energy for the two compound activators  $\text{NaOH} + \text{Na}_2\text{CO}_3$  and  $\text{Na}_2\text{CO}_3 + \text{Ca}(\text{OH})_2$  prove that the value of apparent activation energy depends on the kind of activator and for each of them is equivalent to 35.6 and 60.7  $\text{kJ}\cdot\text{mol}^{-1}$ , respectively. This reliance is a consequence of changes in activation reactions, which are caused by utilizing different kinds of activators.
- Investigations into the order of alkali activation of phosphorus slag show that the rate of activation does not depend on the activator type, and is almost similar to second order reaction. This means that the factor, which controls the alkali-activation kinetics of phosphorus slag, is molecular diffusion.
- The reaction constants, which are calculated on the base of conducted studies on the order of reaction rate, and comparing these values with resulted values from the ASTM C 1074 method indicate that with a good approximation the reaction rate order as well

as reaction constants, and consequently the apparent activation energy can be computed through utilizing compressive strength data of cement mixtures, which are cured at different temperatures.

## REFERENCES

- Torgal F. P., Castro-Gomes J., Jalali S.: *Constr. Build. Mater.* 22, 1305 (2008).
- Torgal F. P., Jalali S.: *Eco-efficient Construction and Building Materials*, ed., Springer, 2011.
- Shi C., Krivenko P. V., Roy D. M.: *Alkali-activated cements and concretes*, ed., Taylor & Francis, London ; New York 2006.
- Wu X., Roy D. M., Langton C. A.: *Cem. Concr. Res.* 13, 277 (1983).
- Haha M. B., Saout G. L., Winnefeld F., Lothenbach B.: *Cem. Concr. Res.* 41, 301 (2011).
- Ravikumar D., Neithalath N.: *Thermochim. Acta* 546, 32 (2012).
- Wang S. D., Scrivener K. L.: *Cem. Concr. Res.* 25, 561 (1995).
- Huanhai Z., Xuequan W., Zhongzi X., Mingshu T.: *Cem. Concr. Res.* 23, 1253 (1993).
- Fogler H. S.: *Elements of chemical reaction engineering*, 5th ed., Prentice-Hall, United States 1986.
- ASTM C1074-98, *Standard Practice for Estimating Concrete Strength by the Maturity Method*, ASTM International, West Conshohocken, PA, DOI:10.1520/C1074-98.
- Oh J. E., Monteiro P. J. M., Jun S. S., Choi S., Clark S. M.: *Cem. Concr. Res.* 40, 189 (2010).
- Lecomte I., Henrista C., Liégeois M., Maserib F., Rulmonta A., Clootsa R.: *J. Eur. Ceram. Soc.* 26, 3789 (2006).
- Sakulich A. R., Miller S., Barsoum M. W.: *J. Am. Ceram. Soc.* 93, 1741 (2010).
- Bonk F., Schneider J., Cincotto M. A., Panepucci H.: *J. Am. Ceram. Soc.* 86, 1712 (2003).
- D'Aloia L., Chanvillard G.: *Cem. Concr. Res.* 32, 1277 (2002).
- Poole J. L., Riding K. A., Folliard K. J., Juenger M. C. G., Schindler A. K.: *ACI Mater. J.* 104, 303 (2007).
- Maghsoodloord H., Khaliliamiri H., Allahverdi A., Lache-mi M., Hossain K. M. A.: *Ceram. Silik.* 58, 227 (2014).
- Shi C., Li Y.: *Cem. Concr. Res.* 19, 527 (1989).
- Qian G., Bai S., Ju S., Huang T.: *J. Mater. Civ. Eng.* 25, 846 (2013).
- ASTM C114-15, *Standard Test Methods for Chemical Analysis of Hydraulic Cement*, ASTM International, West Conshohocken, PA, 2015, DOI: 10.1520/C0114-15.
- ASTM C311 / C311M-13, *Standard Test Methods for Sampling and Testing Fly Ash or Natural Pozzolans for Use in Portland-Cement Concrete*, ASTM International, West Conshohocken, PA, 2013, DOI: 10.1520/C0311\_C0311M-13.
- ASTM C778-13, *Standard Specification for Standard Sand*, ASTM International, West Conshohocken, PA, 2013, DOI: 10.1520/C0778.
- ASTM C109 / C109M-13, *Standard Test Method for Compressive Strength of Hydraulic Cement Mortars (Using 2-in. or [50-mm] Cube Specimens)*, ASTM International, West Conshohocken, PA, 2013, DOI: 10.1520/C0109\_C0109M.
- Fernandez-Jimenez A., Puertas F.: *Cem. Concr. Res.* 27, 359 (1997).
- Pallagi A., Tasi Á., Gácsi A., Csáti M., Pálínkó I., Peintler G., Sipos P.: *Cent. Eur. J. Chem.* 10, 332 (2012).
- Ebbing D. D.: *General Chemistry*, 3 ed., Houghton Mifflin Company, Boston, MA 1990.
- Swaddle T. W.: *Inorganic Chemistry*, ed., Academic Press, San Diego 1997.
- Roy D., Idorn G.: *Am. Concr. Inst. J.* 79, 444 (1982).
- Ezziane K., Bougara A., Kadri A., Khelafi H., Kadri E.: *Cem. Concr. Compos.* 29 587 (2007).
- Schindler A. K.: *Mater. J.* 101, 72 (2004).
- Ma W., Sample D., Martin R., Brown P.: *CCAGPD* 16, 93 (1994).
- Duxson P., Fernandez-Jimenez A., Provis J. L., Lukey G. C., Palomo A., Deventer J. S. J. V.: *J. Mat. S.* 42, 2917 (2007).
- Khale D., Chaudhary R.: *J. Mat. S.* 42, 729 (2007).
- Palomo A., Grutzeck M. W., Blanco M. T.: *Cem. Concr. Res.* 29, 1323 (1999).
- Puertas F., Palacios M., Manzanod H., Doladod J. S., Ricof A., Rodríguez J.: *J. Eur. Ceram. Soc.* 31, 2043 (2011).
- Clayden N. J., Esposito S., Aronne A., Pernice P.: *J. Non-Cryst. Solids* 258, 11 (1999).